

Molecular Mechanism of Field-Inversion Electrophoresis

Jean Louis Viovy

*Laboratoire de Physico-Chimie Structurale et Macromoléculaire, Ecole Supérieure de Physique et de Chimie Industrielle,
75231 Paris Cedex 05, France*

(Received 12 November 1987)

A molecular interpretation is proposed for the strong selectivity of field-inversion electrophoresis, recently applied to the separation of long DNA fragments. The sharp transition in the mobility is associated with an antiresonance occurring when chain-length fluctuations compete with the electrophoretic drift. A theory is outlined based on biased reptation (Slater and Noolandi) and length fluctuations (Doi). Systematic preaveraging allows a simple treatment, and important features of the data are correctly accounted for.

PACS numbers: 82.45.+z, 36.20.Ey, 87.15.-v

The discovery¹ that the separation of very large DNA molecules in agarose gels could be dramatically improved by the use of alternating crossed electric fields has stimulated the development of several pulsed-field electrophoresis techniques.²⁻⁵ In field-inversion gel electrophoresis (FIGE),⁴ pulses of unequal duration are alternately applied along opposite directions. In spite of this beautiful simplicity, a rather complex behavior, including abrupt changes of mobility and nonmonotonic molecular weight (MW) dependences, is observed. I outline a model based on polymer reptation theory,⁶⁻¹² restricting the presentation to a qualitative one in order to enlighten the physical concepts.

A long DNA fragment (or any charged flexible chain) is engaged in a tubelike volume by the uncrossable fibers of the gel. I picture it as a sequence of N "blobs" of size a and charge q , where a is the average pore size of the gel. The motion is restricted to one-dimensional (1D) displacements along the chain's contour. For zero field, only 1D fluctuation modes of the chain are thermally activated: The only mode leading to macroscopic diffusion is the fluctuation mode of order zero, reptation. In the presence of an electric field, the motion of a charged chain is the superposition of fluctuations $f(t)$ with a curvilinear drift due to the field $d(t)$:

$$s(t) = f(t) + d(t). \quad (1)$$

This "biased reptation" process has been described in detail in original papers.^{9,11,13} The instantaneous drift velocity is

$$\dot{d}(t) = F_{\text{eff}}/N\zeta = Eq |R_z|/aN\zeta,$$

where F_{eff} is the effective force on the chain (integrated along the tube path), ζ is the friction per blob, and R_z is the projection of the end-to-end vector onto the field direction. The value of R_z results from a competition between Brownian fluctuations and field bias. As investigated by Slater and co-workers,^{14,15} the chain velocity and R_z are coupled in a nontrivial manner, leading to unexpected effects such as a nonmonotonic MW depen-

dence of the velocity in some constant-field regimes.¹⁵ These complications are ignored here, and a "preaveraged" drift velocity $\dot{d}(t)$ is used:

$$\dot{d}(t) = (Eq/\zeta)(N^{-1/2} + \langle \cos\theta \rangle). \quad (2)$$

The first term represents the preaveraged Brownian contribution to the end-to-end distance. The second term is the average orientation of blobs. In the permanent regime, this orientation is nonzero, because a charged chain end creating a new tube section in the presence of the field preferentially aligns along this field to minimize its energy. For intermediate fields ($Eq/kT < 1$), the orientation is¹¹

$$\langle \cos\theta \rangle_{\infty} = Eq/kT = (N^*)^{-1/2}. \quad (3)$$

It is responsible for a mobility scaling as E^2N^0 for chains longer than N^* (nonlinear regime). I am conscious that (2) is quantitatively incorrect in the "transition domain" $|R_z| \approx a(N^*)^{1/2}$. However, it should be valid in the limit of short and long chains ($N \ll N^*$ and $N \gg N^*$, respectively), and it allows developments on a purely analytical ground, setting the frame for more detailed calculations. Within the preaveraging approximation (PA), the permanent-regime mobility $m_{\infty}(E, N)$, is expressed as

$$m_{\infty}(E, N) = \dot{s} |R_z|/aNE. \quad (4)$$

Consider now a typical FIGE experiment. Starting with a chain in equilibrium, a field $-E_z$ is applied during t_1 . The projection of the end-to-end vector at time 0 onto z defines a "head" A and a "tail" B [Fig. 1(a)]. The chain creates a new tube section AA' with orientation $\langle \cos\theta \rangle_{\infty}$ (counted from A to A') between times 0 and t_1 [Fig. 1(b)]. At this time, the field is inverted during t_2 , exchanging the head and the tail, and the chain further creates a new section $B'B''$, with orientation $-\langle \cos\theta \rangle_{\infty}$ (counted from B' to B''). Therefore, the orientation created at both ends builds up coherently, leading to the same orientation as in the permanent regime. Both "forward" and "backward" motions are ac-

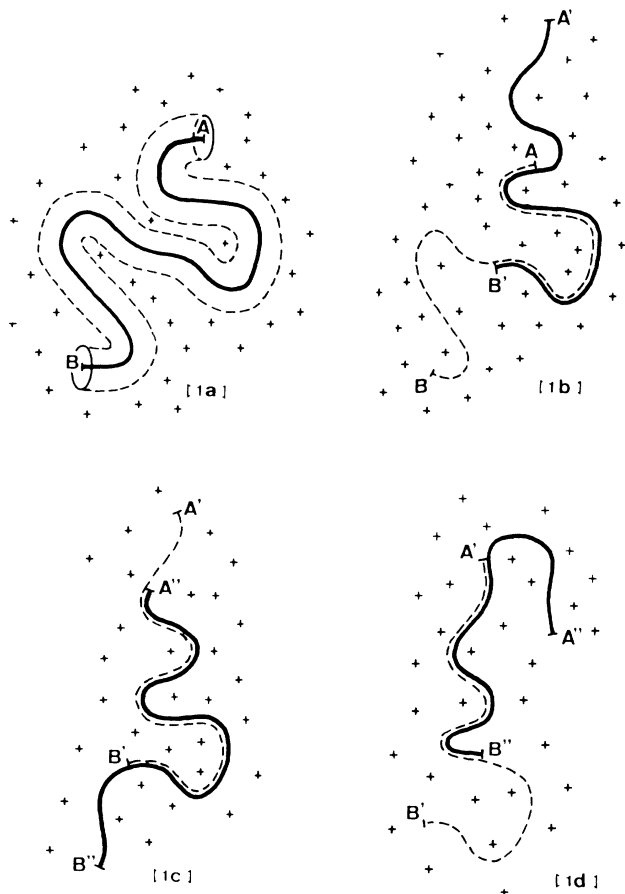


FIG. 1. (a) Schematic description of a chain at rest at $t = 0$ with its "tube." (b) Configuration after application of a field $-Ez$ during t_1 , and (c), (d) after subsequent application of a field $+Ez$ during t_2 [(c) drift dominance, and (d) creation of an ill-oriented section in the case of fluctuation dominance].

celerated by the orientation, and the net mobility is just the macroscopic average

$$m_\infty \cong q\lambda/\zeta N^* \sim E^2 N^0, \quad N \gg N^*,$$

$$m_\infty \cong q\lambda/\zeta N \sim E^0 N, \quad N \ll N^*,$$

with $\lambda = (t_1 - t_2)/(t_1 + t_2)$. This picture breaks down when the alternation times are shorter than the equilibration time of a blob, $T_A = \zeta a^2/kT$. In this case, the field is averaged by the head blob during the creation of a tube section of size a , so that the orientation and the mobility are "effective field" ones, $\langle \cos\theta \rangle = \lambda(N^*)^{-1/2}$ and $m(N \gg N^*) = \lambda^2 m_\infty$, respectively. This change in the orientation shifts the transition between the linear and nonlinear regimes to a higher chain length $N^{**} = N^*/\lambda^2$ but, since T_A does not depend on N , it can account neither for the presence of a sharp "tunable" MW selective band nor for the nonmonotonic MW dependence of the displacement (Fig. 2 in Ref. 4). To understand the "FIGE effect," it is worth while to notice that

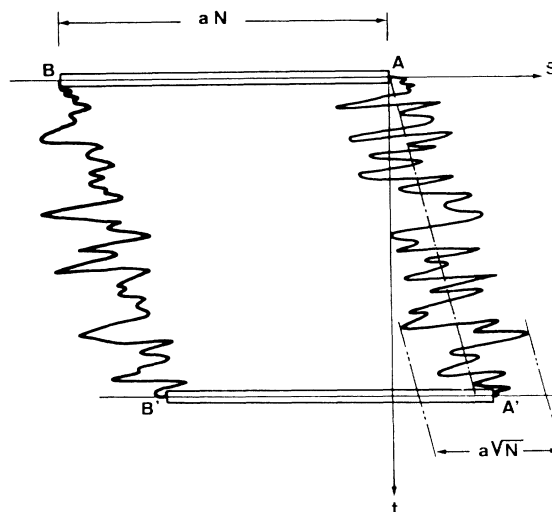


FIG. 2. Schematic evolution of the curvilinear position of chain ends as a function of time (see text). The dashed line is the drift (average value).

the pulse times involved here (typically a few seconds) are generally smaller than those used in orthogonal-field-alternation gel electrophoresis¹⁻³ (typically 1 min for similar chains). This suggests that the process underlying FIGE occurs on a scale larger than a blob, but smaller than the molecule size. Reptation cannot efficiently compete with drift on scales larger than a ,¹⁶ but higher-order modes of fluctuation, called "breathing modes" or "length fluctuations," relax the chain ends rapidly on scales smaller than $aN^{1/2}$. The square-averaged distance relaxed at time t scales as¹²

$$\langle l^2 \rangle \cong a^2 (t/T_A)^{1/2}, \quad t < T_B = N^2 T_A,$$

$$\langle l^2 \rangle \cong a^2 N, \quad t > T_B.$$

Because of the different time exponents of the drift and breathing processes, if one looks at one chain end on a long time scale, the effect of breathing will appear as a "blurring" of chain ends, and the only visible motion will be the continuous drift of the average configuration. On a short time scale, however, many random forward and backward motions will be visible, but the drift will be barely noticeable (see Fig. 2). These two regimes are separated by a critical time T_f [given by $sT_f = a(T_f/T_A)^{1/4}$]. Consider, for instance, a chain at rest when the alternating field is switched on. If $t_1, t_2 \gg T_f$, the net displacement of the end A during t_1 is always positive in regard to the forward direction, and so is that of B . The displacement during a complete backward pulse, and the corresponding orientation, have the opposite direction. This corresponds to the situation represented in Figs. 1(b) and 1(c). If the pulse durations are larger than T_A but smaller than T_f , however, the net displacement of one chain end during the backward pulse, say, involves several blobs, but it can be either positive or negative. In

other words, fluctuations, which dominate on that time scale, may have imposed that A play the role of a head "against" the field. In such a case, the segments created are oriented along the field acting at the moment of their creation, inducing "ill-oriented" tube sections [Fig. 1(d)]. Because of the stochastic nature of this process, not all the ill-oriented segments will be visited again, and these trapped segments reduce the overall orientation of the chain.

To relate the average orientation of "head sections" created at time t , $\langle \cos\theta \rangle_t$, with the instantaneous drift velocity, I use a preaveraging approximation again. I suppose that during t_1 , one half of the chains has moved

$$\langle \cos\theta \rangle_t = \langle \cos\theta \rangle_\infty \{1 - \text{Pos}[\text{Pos}(f_2 - d_2) - \text{Pos}(f_1 - d_1)] / (d_1 - d_2)\}. \tag{5}$$

A minimal set of dimensionless parameters is introduced: $\phi = f_1/d_1$ reflects the balance between drift and fluctuations on a time scale t_1 , $\rho = t_2/t_1$ is the pulse asymmetry parameter, and $\nu = (N^*/N)^{1/2}$ is related to the chain length. Then the "instantaneous" orientation η_t is expressed in a reduced form:

$$\eta_t = \langle \cos\theta \rangle_t (N^*)^{1/2} = 1 - \text{Pos}[\text{Pos}(\phi\rho^{1/4} - 1) - \text{Pos}(\phi - 1)]. \tag{6}$$

Figure 3 displays the evolution of η_t as a function of ϕ^{-1} (increasing drift velocity). An "antiresonance dip" appears around 1 because the probability of the creation of an ill-oriented segment decreases with the drift velocity, but the probability that it will be trapped increases with it. The joint probability is maximum when fluctuation and drift distances are similar. The unphysically sharp angles are a consequence of the simplifications. This result is not directly useful, because η and η_t are related in a rather complicated manner: With use of (1) and (2), ϕ is expressed as $\phi_0/(\nu + \bar{\eta})$, where $\phi_0 = (T_A/t_1)^{3/4}N^*$, and $\bar{\eta}$ is the reduced orientation averaged over all segments of the chain regardless of their creation

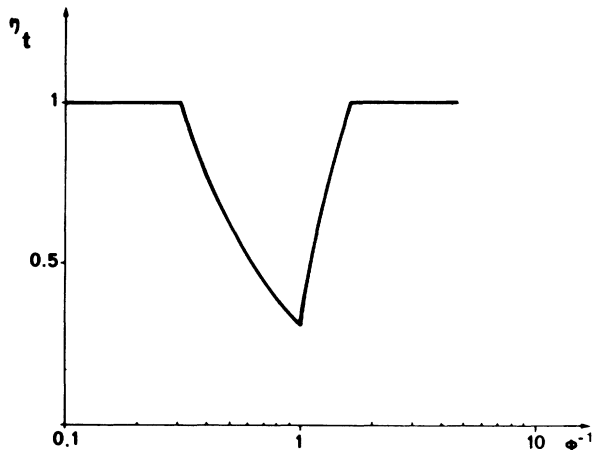


FIG. 3. Evolution of η_t as a function of ϕ .

$d_1 + f_1$, and the other half has moved $d_1 - f_1$. d_1 and f_1 are the average drift distance st_1 and the average fluctuation distance $a(t_1/T_A)^{1/4}$, respectively. In the same way, all possible displacements during t_2 are replaced by equally probably displacements $-d_2 + f_2$ and $-d_2 - f_2$. This approximation seems very crude, but it should be reasonable here because of the exponent of $\frac{1}{4}$ in f . The number of ill-oriented segments created during the t_2 pulse is then approximated as $0.5\text{Pos}(f_2 - d_2)$, where Pos means positive part (if drift dominates, no ill-oriented segment is created). One must also account for the number of segments destroyed by fluctuations during the next pulse t_1 , $0.5\text{Pos}(f_1 - d_1)$. Finally,

time. $\bar{\eta}$ plays the role of a memory term depending on the history of η_t . Locally stable stationary solutions ($\eta = \bar{\eta}_t$) are represented in Fig. 4 as a function of ν and for different values of ϕ_0 . For $\phi_0 < \phi_f = (1 - \rho^{1/4}) / (1 - \rho)$, i.e., $(t_1/T_A) > (\phi_f N^*)^{4/3}$, a single solution $\bar{\eta} = 1$ is obtained for all values of ν . If $\phi_0 > \phi_f$, two cases are obtained depending on ν : For $\nu > \nu_f = \phi_0 = \phi_f$, the single solution $\bar{\eta} = 1$ is recovered, but two self-consistent solutions exist if $\nu < \nu_f$ [ν_f corresponds to a critical chain size $N_f = N^* / (\phi_0 - \phi_f)^2$]. The minimum of the orientation, $\bar{\eta}_f = \phi_f$, is obtained for N_f .

I did not consider here the absolute "stability" of the two solutions in the bistable regime, a problem out of the reach of the preaveraged theory, but the evolution of a chain at rest ($\bar{\eta} = 0$) when the pulsed field is applied, computed in the PA, provides some insight into the importance of this stability problem. For this, I solve numerically a discretized version of (6). $\bar{\eta}$ converges towards a finite value $\bar{\eta}_\infty$, plotted in Fig. 4. The balance

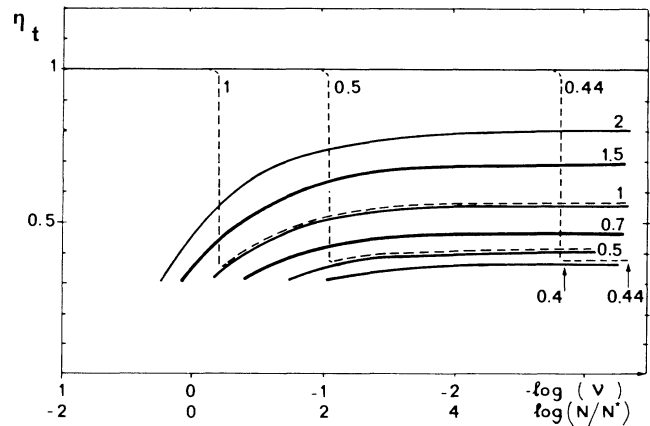


FIG. 4. Orientation for different chain lengths and different values of ϕ_0 (indicated on the lines). $t_1 = 2t_2$. Stationary solutions, full lines; convergence value for an initially nonaligned chain, dashed lines.

between the stability region of the "slow" solution, which narrows for decreasing ϕ_0 , and the oscillations in the orientation induced by the retarded nature of (6) induces a nontrivial "choice" between the solutions. For ϕ_0 larger than a critical value $\phi_c \approx 0.44$, a sharp decrease of $\bar{\eta}_\infty$ occurs, leading to a sharp decrease of the mobility [according to (2) and (4), the mobility scales as $\bar{\eta}_\infty^2$] at a value of the chain length increasing with the pulse times (decreasing ϕ_0). This fact, and the predicted value of the mobility reduction (a factor about 10 for $\rho=0.5$), are in agreement with experiments.⁴ It is also worth noticing that, beyond a finite value of ϕ_0 , $\bar{\eta}$ converges towards 1 for all chain lengths. Practically, this corresponds to an absolute upper limit to the separable chain lengths, appearing at finite pulse times. This prediction also seems in agreement with experiment. This is certainly not the whole story of FIGE: On the theoretical side, the relevance of (2) and (3) for actual experiments is still under discussion.¹⁷ On the experimental side, the present PA model predicts a nonmonotonic dependence of the orientation as a function of N , but its variation is too weak to account for the sharp increase of the mobility observed in some experiments (see, e.g., Fig. 2 in Ref. 4). I expect that the experimental nonmonotonic behavior is related with nontrivial averaging, as in the case of continuous field.¹⁵ However, the qualitative agreement of this model with other features of the available experiments justifies further efforts in the direction.

This work was partly supported by Ministère de la Recherche et de l'Éducation Supérieure (France) Grant

No. 87C0186. I acknowledge fruitful discussions with H. Hervet, F. Caron, and G. Thomas.

-
- ¹D. C. Schwartz and C. R. Cantor, *Cell* **37**, 67 (1984).
 - ²G. F. Carle and M. V. Olson, *Nucleic Acid Res.* **12**, 5647 (1984).
 - ³C. L. Smith and C. R. Cantor, *Nature (London)* **319**, 701 (1986).
 - ⁴G. F. Carle, M. Frank, and M. V. Olson, *Science* **232**, 65 (1986).
 - ⁵G. Chu, D. Vollrath, and R. W. Davis, *Science* **234**, 1582 (1986).
 - ⁶P. G. de Gennes, *J. Chem. Phys.* **55**, 572 (1971).
 - ⁷L. S. Lerman and H. L. Frisch, *Biopolymers* **21**, 995 (1982).
 - ⁸O. J. Lumpkin and B. H. Zimm, *Biopolymers* **21**, 2315 (1982).
 - ⁹G. W. Slater and J. Noolandi, *Phys. Rev. Lett.* **55**, 1579 (1985).
 - ¹⁰O. J. Lumpkin, P. Dèjardin, and B. H. Zimm, *Biopolymers* **24**, 1573 (1985).
 - ¹¹G. W. Slater and J. Noolandi, *Biopolymers* **24**, 2181 (1985).
 - ¹²M. Doi, *J. Polym. Sci., Polym. Lett. Ed.*, **19**, 265 (1981).
 - ¹³J. L. Viovy, *Biopolymers* **26**, 1929 (1987).
 - ¹⁴G. W. Slater, J. Rousseau, and J. Noolandi, *Biopolymers* **26**, 863 (1987).
 - ¹⁵J. Noolandi, J. Rousseau, G. W. Slater, C. Turmel, and M. Lalande, *Phys. Rev. Lett.* **58**, 2428 (1987).
 - ¹⁶J. L. Viovy, *C. R. Acad. Sci. Ser. 2*, **305**, 181 (1987).
 - ¹⁷J. Deutsch, *Phys. Rev. Lett.* **59**, 1255 (1987).